Detecting Land Use Land Cover Changes Induced by the Dynamics of River Indus, Pakistan, from 1972 -2022, Using Remote Sensing and GIS Techniques

Hameed Ullah Khan, Abu Bakkar, Junaid Ullah Khan Aman, Dr. Ihsan Ullah Khattak
Department of Geography and Geomatics University of Peshawar
***Correspondence:** hameedstark10@gmail.com, Abubakkariqbal09@gmail.com, jukabbangash6058@gmail.com, Ihsanullah@uop.edu.pk

Citation | Khan. H. U, Bakkar. A, Aman. J. K. A, Khattak. I. U, "Detecting Land Use Land Cover Changes Induced by the Dynamics of River Indus, Pakistan, from 1972 -2022, Using Remote Sensing and GIS Techniques", IJIST, Special Issue pp. 714-732, July 2024
Received | June 26, 2024 **Revised |** July 02, 2024 **Accepted |** July 09, 2024 **Published |** July 13, 2024.

Introduction/Importance of the Study:

This study investigates the shifting patterns of the Indus River and its consequent impact on land use and land cover (LULC) over a 50-year period, from 1972 to 2022, using Geographic Information System (GIS) and Remote Sensing (RS) techniques. The research is crucial for understanding the dynamics of river behavior and its broader implications for flood management and land use planning.

Novelty Statement:

This research uniquely explores the complex relationship between river shifting and LULC changes, offering fresh perspectives on managing flood risks and optimizing land use. The study emphasizes the significant economic impact of chronic alluvial erosion caused by the river's rapid flow, which has perpetuated poverty among local residents and resulted in substantial annual national asset losses.

Materials and Methods:

The study utilized satellite imagery spanning from 1972 to 2022, applying GIS and remote sensing techniques to analyze the Indus River's sinuosity, channel migration, erosion, and accretion patterns, as well as LULC changes. Key methodologies included calculating the river's sinuosity index, assessing channel and bank migration, and employing the Normalized Difference Water Index (NDWI) alongside maximum likelihood classification for precise LULC assessment.

Results and Discussion:

The long-term analysis revealed that river erosion significantly influenced land areas, leading to an expansion of settlement areas, a reduction in vegetation, and fluctuations in barren land, water bodies, and agricultural land. Built-up areas expanded markedly, indicating population growth within floodplains. Erosion and deposition processes notably impacted agricultural and settlement areas, contributing to socio-economic stress and triggering internal migration. Satellite images captured during the spring and dry seasons (March to May) indicated minimal stream flow due to reduced rainfall. The study identified critical management zones—Reaches A, B, C, H, I, and J—where erosion was most pronounced from 1972 to 2022. Minor embankment improvements are recommended for these reaches, as initial migration occurred on the right side in Reaches A, B, and C, shifted to the left from D to G, and affected both sides from H to J.

Concluding Remarks:

This research underscores the vital role of GIS and remote sensing in analyzing river dynamics and their effects on land use. The findings provide essential insights for informed decision-making in flood management and land use planning, ultimately contributing to better resource management and community resilience.

Keywords: Indus River Shifting, Land Use and Land Cover (LULC), Geographic Information System (GIS), Remote Sensing (RS), Erosion and Accretion Patterns, Flood Management, Socio-Economic Impact.

Introduction:

The Indus River, one of the largest rivers in the world, originates from Mount Kailas and flows through the Ladakh Himalaya. Its hydrological budget is primarily derived from melting glaciers, westerlies, and the Indian Summer Monsoon (ISM), with most floods occurring during the ISM precipitation regime. Rivers are vital for both human societies and ecosystems, yet they can also cause significant damage during floods, leading to the loss of crops, property, and lives [1]. Before reaching the Indus Fan, fourteen major tributaries contribute to its discharge and sediment load [2]. The ecological equilibrium and hydromorphologic symmetry of the riverine environment are directly influenced by both natural and anthropogenic factors. The current research aims to analyze the hydromorphologic features—such as meanders, shape, and size—of the Indus River in Pakistan using remote sensing (RS) and Geographic Information System (GIS) techniques to evaluate temporal changes [3]. The Indus River, which is the main tributary of Pakistan, starts in the northern region and ends in the Arabian Sea. Downstream of Panjnad, near Mithankot, five major rivers from the east (Jehlum, Chenab, Ravi, Beas, and Sutlej) merge with the Indus River, collectively contributing sediment flux to the Arabian Sea [3].

Despite the dynamic nature of the Indus floodplain, which shows abundant traces of intense and continuous human activity, erosion and sedimentation processes typical of these changing floodplains have significantly impacted the preservation and interpretation of archaeological remains. These continuous transformations pose challenges for Remote Sensing (RS) applications in studying past landscape dynamics. Initially, RS was more effective in areas with long-term soil stability, such as the Middle East and northern Europe, where historical traces are often preserved within present-day landscapes [4]. However, in the expansive Indus region, RS has been extensively used to locate vanished rivers and explore their relationship with ancient and historical settlements. RS has supported geoarchaeological and archaeological surveys, particularly in the Yamuna–Sutlej interfluve in northwestern India and the arid region now occupied by the ephemeral Ghaggar-Hakra River, which has been a focus of historical and recent research [5]. The morphology of a river thalweg in a deltaic environment is continuously reshaped by the interaction between fluvial and marine hydrodynamic processes. Fluvial flow parameters, such as volume and flow velocity, contribute to the widening of the thalweg and the development of a braided pattern in the river course within a delta region [6].

Indus River Geography:

The Indus River, stretching over 1,800 miles, is a vital artery of the Indian subcontinent, holding a significance comparable to that of the Ganges. Flowing through semi-arid regions, the river boasts an annual flow volume twice that of the Nile. For more than 4,000 years, the Indus has served as a natural boundary, a critical source of agricultural irrigation, and a cultural heartland. Originating in Tibet, the river flows northwest through Kashmir, skirting the southern edge of the Karakoram Mountains, before entering Pakistan, where it forms the Tarbela Reservoir. As it continues its journey, the Indus flows into the plains of Punjab and Sindh, where it broadens and splits into smaller channels before ultimately reaching the Arabian Sea. Passing by Hyderabad, the river concludes its course in a significant delta southeast of Karachi.

The Indus River's tributaries—including the Jhelum, Chenab, Ravi, Beas, and Sutlej Rivers—are essential for supporting agriculture across the region. Over half of Pakistan's population resides along the Indus River valley, relying on its waters for irrigation, drinking water, and various other needs. Major cities such as Faisalabad, Lahore, Rawalpindi (Islamabad), and Peshawar are heavily dependent on the resources provided by the Indus [7]. Geological and geophysical studies indicate that the Indus River system was initiated shortly after the collision between the Indian and Eurasian Plates during the Middle Eocene. The geology of the Indus drainage basin has been profoundly influenced by this tectonic collision, which began around 50 million years ago and has since shaped the landscape of the region [8].

Materials and Methods:

Study Area:

The study focuses on the section of the Indus River that stretches from Sukkur to Laila, encompassing the region approximately bounded by the coordinates 25° 12' 05" N to 26° 45' 52" N latitude and 69° 24' 44" E to 68° 57' 32" E longitude. This area is represented on Pakistan's topographic sheet number 39 (Figure 1).

Data Collection:

Acquisition of Data: This study employs satellite imagery from the United States Geological Survey (USGS) for the years 1972, 1979, 1992, 2012, and 2022 to examine the Indus River's migration patterns, sinuosity, erosion, and accretion processes. A 30-kilometer buffer zone was established around the river's centerline to facilitate the development of detailed land use and land cover (LULC) maps. Comprehensive graphs and visualizations were generated to compare temporal data, thereby enhancing the clarity and robustness of the study's findings.

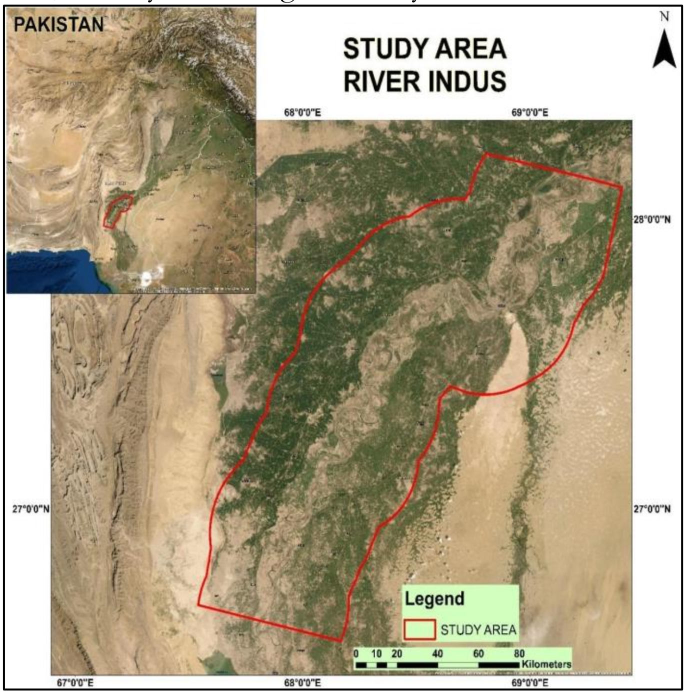

Figure 1: Study Area

Data Source:

To reconstruct channel movement and analyze land use and land cover (LULC) changes, this study integrates satellite imagery with Geographic Information System (GIS) techniques. Remote Sensing (RS) and GIS are employed to delineate river features, examine river dynamics, and assess their impact on land use. The study relies on secondary data, including satellite images and information from various online sources, to conduct a comprehensive analysis of the river's behavior and its influence on the surrounding landscape.

Methodology:

The methodology for this study includes the following detailed steps:

Data Collection:

Landsat images were downloaded from the USGS Earth Explorer for various time periods: 1972, 1979, 1992, 2002, 2012, and 2022. Specifically, Landsat 1 images were utilized for 1972, Landsat 3 for 1979, Landsat 5 for 1992, Landsat 7 for both 2002 and 2012, and Landsat 9 for 2022.

Extraction of the Indus River:

After data collection, the primary objective was to extract the Indus River from the Landsat images to calculate channel migration, assess sinuosity, and analyze erosion and accretion over the years. The extraction process utilized the Normalized Difference Water Index (NDWI), calculated as (Green - NIR) / (Green + NIR), to differentiate water bodies from the surrounding land. ISO Cluster Unsupervised Classification, along with Arc Toolbox, was employed to isolate the river. This approach successfully extracted the Indus River, enabling detailed analysis of its dynamic changes over time.

Calculating Channel Migration and Sinuosity:

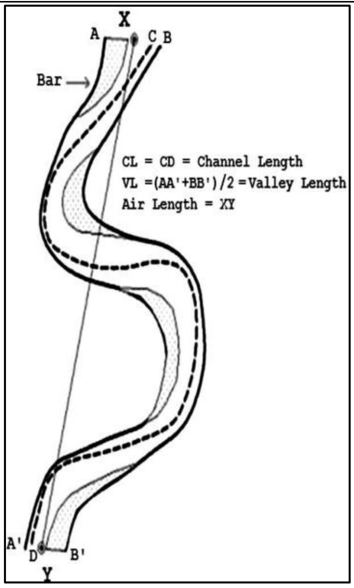

Figure 2: Sinuosity index evaluation system [9]

Stream sinuosity indexes are usually derived by dividing the length of a river reach as measured along the channel by the length of the same reach as measured along the valley [10]. To calculate river migration over time, the centerline for each year's river path was determined using the "Collapse Dual Line to Centreline" tool, with the 1972 centerline as the reference. Sinuosity, which reflects the ratio between the actual river length and the straight-line valley length, was assessed using this index. The entire stretch of the Indus River from Sukkur to Laila was divided into 10 reaches (Figure 3). For channel migration analysis, each reach was further subdivided into 8 segments (Figure 4), and migration was measured in meters.

Calculating Erosion and Accretion:

To assess erosion and accretion, the area of the river for each year was calculated using the “Calculate Geometry” function. The 1972 river served as the reference, and subsequent river shapes were intersected with the 1972 river using the intersect tool. Fields for unchanged area, erosion, and accretion were created in the attribute table. Erosion was determined by subtracting the unchanged area from the area of the previous year, while accretion was calculated by subtracting the unchanged area from the area of the next year.

Land Use Land Cover:

A 30 km buffer zone around the river was established, and the study area was extracted using the "Extract by Mask" tool. To facilitate sample selection, data from all years were displayed as true color composites. Supervised classification was then employed to categorize the land into six classes: Water Body, Built-up Area, Agricultural Land, Vegetation, Barren Land, and Uncultivated Land.

Land Use Land Cover Change:

Land-use and land-cover (LULC) change is a crucial component in contemporary strategies for monitoring environmental changes and managing natural resources [11]. Increasing anthropogenic activities are leading to significant alterations of the Earth's surface, which impact global systems [12]. The primary objective of this study is to detect LULC changes over the years using supervised image classification, with the 1972 LULC layer as a baseline. Raster images were converted to polygons and merged into single features using the Dissolve Tool. The area for each year 1979, 1992, 2002, and 2012 was calculated in square kilometers. Changes between years were identified using the Intersect tool, and fields for “Change” and “Area Change” were added to the attribute table. The “Change” field was calculated by comparing the class of the previous year with the class of the next year, highlighting features that transitioned from one class to another. The data was analyzed in Excel, and graphs were created to enhance the analysis. A comprehensive map layout was prepared to visualize the results effectively.

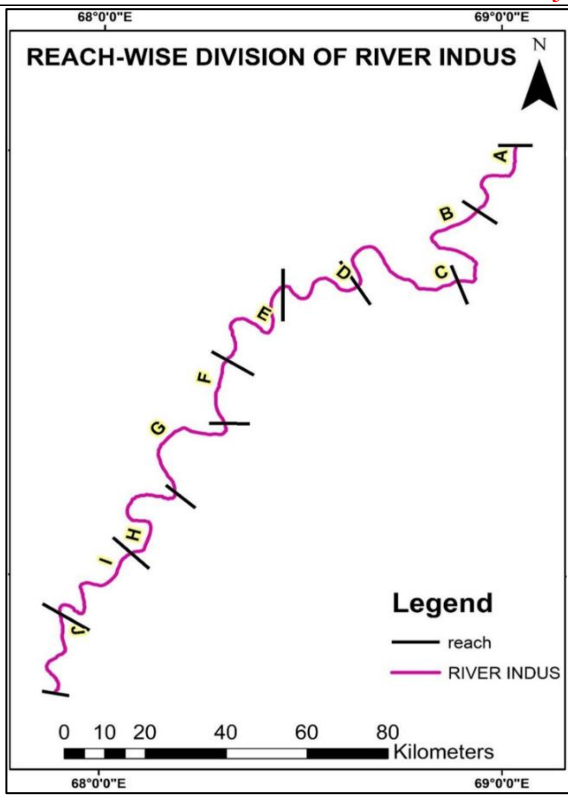

Figure 3: Reach Division of River Indus

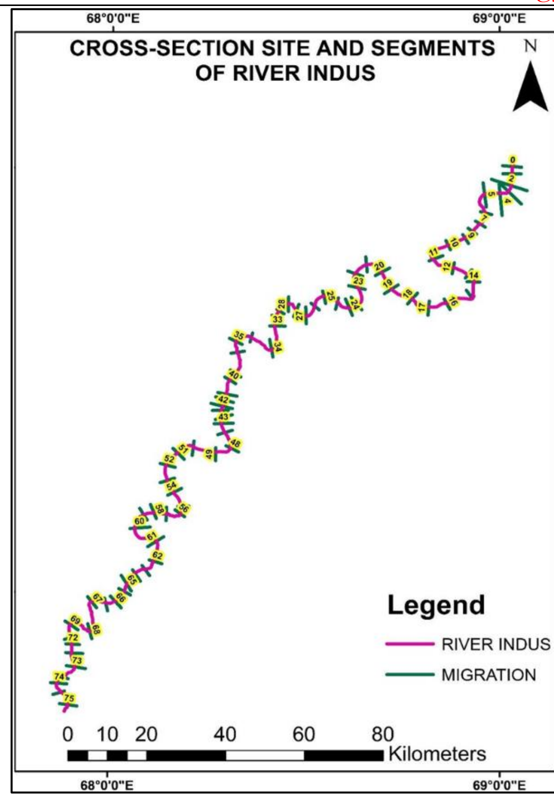

Figure 4: Cress Section site and Segments of river Indus

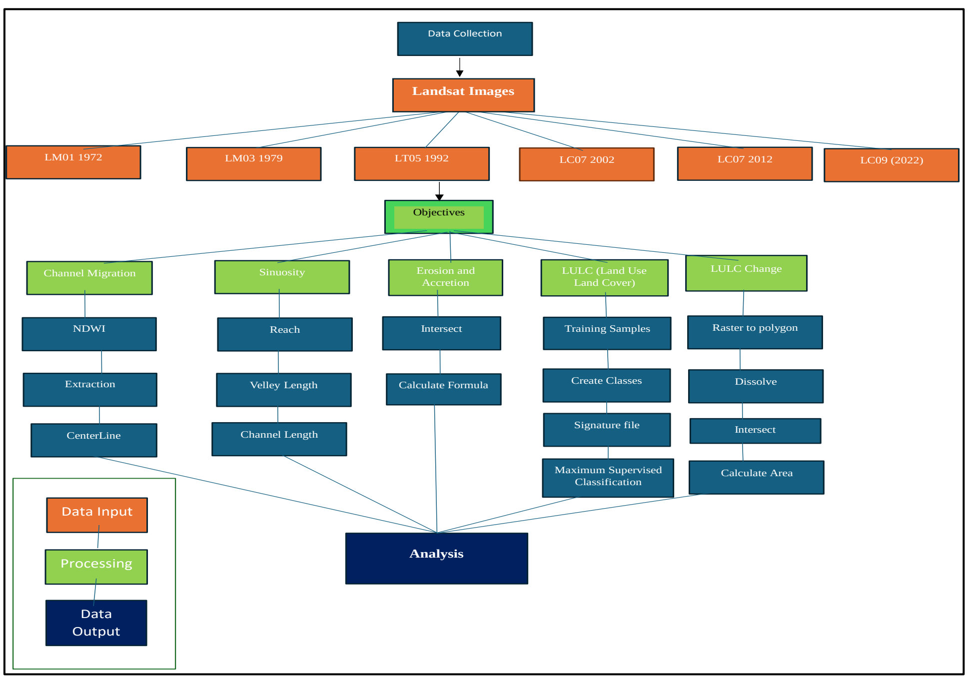

Figure 5: Methodology Adopted

Result:

Behavior Analyses of River Indus:

The analysis of the Indus River's shifting and impact assessment was conducted from 1972 to 2022, with 1972 serving as the baseline. This study examined various aspects, including river sinuosity, erosion and accretion, channel migration, riverbank shifting, and the dynamics of channel and meander belts using satellite images. The Normalized Difference Water Index (NDWI) was employed to reconstruct river boundaries. The river's centerline was digitized from 1972 to 2022 and overlaid to assess shifting characteristics along a 306 km stretch, divided into 10 reaches. The mid-channel and overall channel lengths were measured to calculate sinuosity, as described by [13].

$$\mathbf{P = L_{cmax} / LR}$$

Where Lcmax = Length of midline (single channel); and LR = overall length between two reaches. Erosion and accretion were detected using the difference between the left and right bank migration areas:

EoA = EA - DA

EoA denotes erosion or accretion, with EA representing the erosional area and DA the depositional area. For assessing the impact of river migration, corrected satellite images were utilized to extract a 30 km buffer from the main channel for the year 2022. Six land-use and land-cover (LULC) classes were identified from Landsat images: cultivated land, vegetation, water, barren land, uncultivated area, and built-up area, using the maximum likelihood supervised classification technique. Vegetation was predominantly located near settlement areas and exhibited specific alignment patterns [14].

River Sections:

The lengths of the channel centerlines were 306 km for 1972, 321 km for 1979, 336 km for 1992, 333 km for 2002, 315 km for 2012, and 336 km for 2022. Ten reaches were identified for each mid-channel measurement, except for the periods 1972-1979 and 1979-1992, due to the unavailability of satellite images.

River Sinuosity:

Meandering is a natural geomorphic process resulting in the gradual migration of a river's course and the erosion of its banks [15]. Historical analysis of the River Indus's meander bends reveals a decrease in meandering tendencies over time. Sinuosity calculations show higher values in the initial reaches compared to the downstream reaches. In 1972, the maximum sinuosity was 1.9 at reach B, while the lowest was 1.1 at reach F, with an average of 1.5. By 1979, the maximum sinuosity increased to 2.1 at reaches D and G, with the lowest value remaining at 1.1 at reach I, and an average of 1.6. In 1992, the highest sinuosity was 2.7 at reach F, and the lowest was 0.9 at reach I, with an average of 1.7. By 2002, the highest sinuosity was 2.0 at reach F, and the lowest was 1.3 at reach I, with an average of 1.6. In 2012, the maximum sinuosity was 1.9 at reach B, and the minimum was 1.2 at reach C, averaging 1.5. In 2022, the highest sinuosity was 1.9 at reach E, and the lowest was 1.1 at reach B, with an average of 1.5 (Table 1). Higher sinuosity values indicate a greater rate of lateral migration, unstable lithology, and sediment deposition. The maximum sinuosity value of 2.7 was recorded at reach F in 1992, while the minimum value of 0.9 was at reach I in 1992. According to the sinuosity index, channels are classified as straight (SI < 1.05), sinuous (SI 1.05–1.5), and meandering (SI > 1.5). The River Indus, in the study area, can be classified as a meandering river.

Table 1: Showing the sinuosity values of the reaches

Reaches	SINUOSITY 1972	SINUOSITY 1979	SINUOSITY 1992	SINUOSITY 2002	SINUOSITY 2012	SINUOSITY 2022
A	1.3	1.2	1.8	1.5	1.5	1.3
B	1.9	1.9	1.4	1.7	1.9	1.1
C	1.7	1.4	1.9	1.8	1.2	1.6
D	1.3	2.1	2.5	1.4	1.5	1.8
E	1.5	1.5	0.9	1.3	1.6	1.9
F	1.1	1.4	2.7	2.0	1.6	1.3
G	1.6	2.1	1.2	1.7	1.3	1.7
H	1.8	2.0	1.6	1.6	1.8	1.3
J	1.2	1.2	1.7	1.5	1.4	1.6
I	1.4	1.1	1.1	1.3	1.3	1.4
Average	1.5	1.6	1.7	1.6	1.5	1.5

Erosion and Accretion:

The analysis of erosion and accretion along the River Indus from 1972 to 2022 revealed notable variations. The highest erosion was observed between 1972 and 1979 on the left bank, totaling 378.7 km. In contrast, the most significant accretion occurred between 1979 and 1992 on the right bank, amounting to 153.9 km. Between 1992 and 2002, erosion was 176.5 km, while accretion reached 99.4 km. The period from 2002 to 2012 experienced the lowest levels of erosion (95.6 km) and accretion (115.6 km). From 2012 to 2022, erosion increased to 155.9 km, with the lowest accretion of 97.3 km observed on the right bank. These findings highlight the dynamic nature of river processes over the decades, significantly influencing the stability and morphology of the riverbanks (Figure 6).

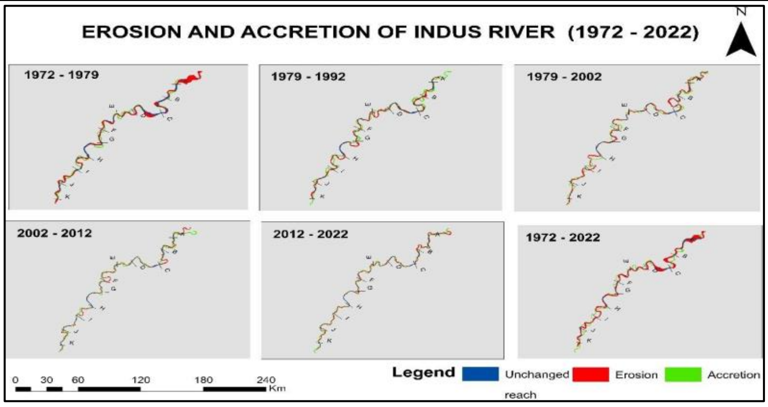

Figure 6: Map showing erosion and accretion of River Indus 1972-2022

Channel Migration (Centreline Migration):

River shifting rates and directions have been identified numerically and are shown in Fig. 6a–e. To calculate the River Indus migration rate and direction, 1972 was used as the baseline. Each reach was divided into eight sections, totaling 80 sections. From 1972 to 1979, the maximum migration distance was 5798 m on the left bank of reach C, and the minimum was 4 m at reach G. In 1992, the maximum was 4982 m on the left bank of reach I, and the minimum was 74 m at reach E. In 2002, the maximum was 8865 m on the left bank of reach B, and the minimum was 11 m at reach F. By 2012, the maximum was 10636 m on the left bank of reach B, and the minimum was 11 m at reach C. In 2022, the maximum was 10890 m on the left bank of reach B, and the minimum was 4 m at reach C. Migration on the initial reaches A, B, and C was to the right side but shifted to the left from D to G. In the later reaches H to J, the river channel shifted both left and right. Overall, the maximum channel migration from 1972 to 2022 occurred in 2022 on reach B (10890 m), while the minimum was in 1992 and 2022 at reaches G and C (4 m) (Figure 7, and table 3).

Table 2: Shows the values of erosion and accretion from 1972-2022

Years	Previous Year Area (sq. km)	Next Year Area (sq. km)	Unchanged Area (sq. km)	Erosion	Accretion
1972 -1979	485	230.3	106.3	378.7	124.0
1979 - 1992	230.3	205.2	51.3	179.0	153.9
1992 - 2002	205.2	128	28.6	176.5	99.4
2002 - 2012	128	148.1	32.5	95.6	115.6
2012 - 2022	1481	129.4	32.2	115.9	97.3
1972 - 2022	485	129.4	42.8	442.2	86.6

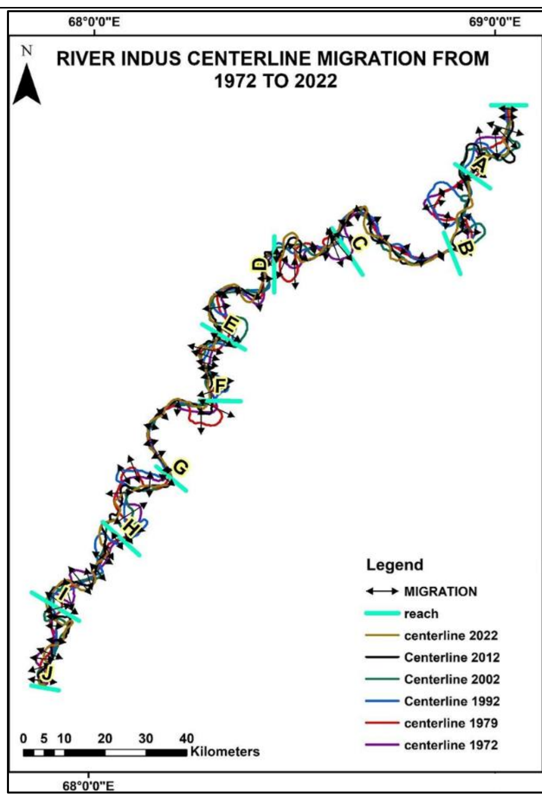

Figure 7: Showing the centerline migration of River Indus

Table 3: Shows the values of channel migration at specific reaches from 1972- 2022, negative values are for the left lateral direction.

REACH	NAME	1979	1992	2002	2012	2022
A	S1	-366	-866	436	550	349
	S2	166	-500	1084	855	658
	S3	231	576	-132	1090	-2221
	S4	916	1753	6155	2965	10
	S5	1648	4190	5444	7250	4652
	S6	2928	1096	2742	5592	3936
	S7	-335	-1915	-3712	-271	-698
	S8	1020	-2275	-3288	-3647	-812
B	S9	159	-986	-1591	-2406	506
	S10	-500	4190	3122	4421	5931
	S11	190	-2562	4916	6922	6645
	S12	2521	1309	8865	10636	10890
	S13	-855	-2366	5980	3482	2974
	S14	1267	2780	-829	472	-1244
	S15	580	1574	3858	-1972	-3126
	S16	-123	-1023	-990	-4532	-4439
C	S17	164	105	20	-11	4
	S18	367	441	1054	928	1579
	S19	748	-652	1754	2255	3324
	S20	275	585	887	1145	-206
	S21	604	-670	720	724	2373
	S22	-4943	-1023	-1256	-1133	-994
	S23	-356	-1085	-566	-117	-663
	S24	-2533	-1670	-3333	-2869	-2799
D	S25	-5798	-3953	-5435	-5741	-4117
	S26	-308	-3773	-4472	-4737	2625
	S27	-2699	-1654	-1425	-425	1146
	S28	-4324	230	2142	2555	-8490
	S29	-617	-1909	-3370	1486	1559
	S30	2678	-3753	-5622	-7435	-7162
	S31	-3670	-3014	-4260	-5830	-1420
	S32	-5633	-2755	-1750	743	-4421
E	S33	-348	860	-1274	-864	-1185
	S34	260	-90	-211	-492	553
	S35	-1619	1356	1290	68	-2626
	S36	-789	-3665	-3027	-2198	-1020
	S37	2144	-74	328	-679	-154
	S38	207	-1338	-1248	-300	-34
	S39	-1063	-2291	-2775	-3473	-3515
	S40	199	3095	2487	-2203	-897
F	S41	2697	4073	5565	1114	556

	S42	-2074	-818	-1703	-2990	-3419
	S43	-1441	-992	-2027	-2982	-1477
	S44	2184	-1324	-2095	-1748	446
	S45	171	-974	46	-695	-310
	S46	-34	2082	1088	701	-488
	S47	-2490	4768	-403	1180	-3399
	S48	1479	4515	6	-300	168
	S49	4	-2907	-2756	-1362	-2415
	S50	2516	-2117	-1781	-290	-1109
	S51	-714	-932	-400	-1712	-2008
G	S52	-380	-404	-611	-471	-399
	S53	-95	305	197	-198	-373
	S54	-290	-248	-512	-588	-622
	S55	-128	-217	-359	-13	31
	S56	804	143	698	838	1021
	S57	820	-890	1861	1770	1916
	S58	2952	-1163	2977	2043	1901
	S59	-2324	-1488	3751	3627	2616
H	S60	-1459	-2594	2483	2864	3338
	S61	-220	2697	2075	888	1407
	S62	-2764	-4495	-1940	-5268	-4903
	S63	665	1363	-1692	-7098	-5404
	S64	79	698	-5100	-6133	-5085
	S65	-261	721	-4258	-5463	-5559
	S66	-1371	-4982	-1938	-1462	-358
	S67	-71	-2728	-1755	-1440	-1099
I	S68	3570	1008	1345	-347	5729
	S69	-3544	1482	1531	3172	-5761
	S70	3491	3657	2966	4188	-112
	S71	1881	-3287	-4647	-5050	3625
	S72	-1321	480	945	197	-867
	S73	444	515	-964	-37	-217
	S74	374	1089	-1890	259	1862
	S75	1871	1422	3980	-4320	2090
	S76	-906	335	1062	-79	-2064
J	S77	-166	2299	2780	2422	4144
	S78	1580	3417	3821	3974	427
	S79	-134	1979	1160	1760	2173
	S80	2828	-834	-2100	-2328	-615

River Bank Migration:

The analysis of lateral direction and riverbank migration along the River Indus from 1972 to 2022 reveals diverse dynamics across different reaches. In the initial reaches, A and B, migration predominantly occurs on the right bank, while in the mid reaches, C to G, left bank migration is more prevalent. In the end reaches, H to J, migration is observed on both banks. Between 2002 and 2022, reach B section 12 exhibited the highest right bank migration, increasing from 10,275 m to 10,443 m. In contrast, the minimum migration was recorded from 2002 to 2012 at reach B section 14 (17 m) and from 2012 to 2022 at reach B section 9 (9 m). These findings suggest significant instability in the riverbanks, with varying migration patterns across different reaches. Overall, reaches A and B primarily experience right bank migration, reaches C to G show left bank migration, and the river exhibits a general leftward migration trend (Figure 8).

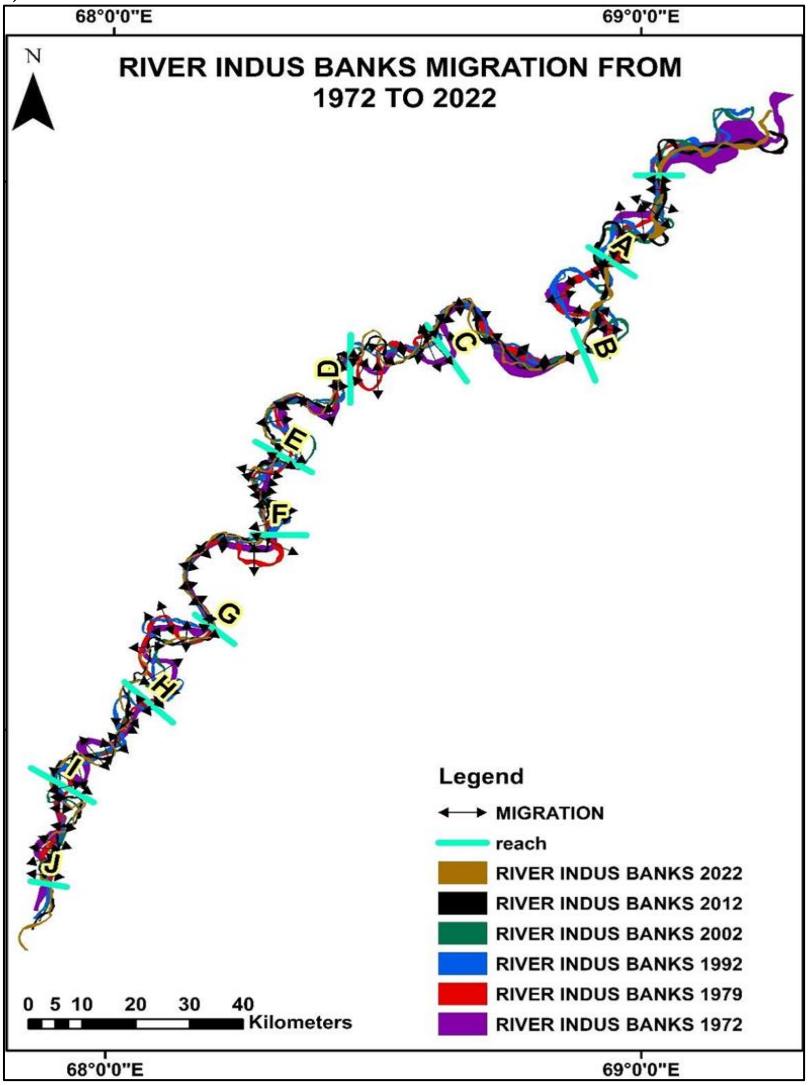

Figure 8: Map showing River Indus Banks Migration 1972-2022

Table 4: shows the values of banks migration at specific reaches from 1972- 2022, negative values are for the left lateral direction

REACHES	SECTION	BANK 1979	BANK 1992	BANK 2002	BANK 2012	BANK 2022
A	S1	-1439.5	-1648	-497.5	-109	-63.5
	S2	-831	-1343	556.5	612	378
	S3	-995	-442	-1249.5	397.5	-2470
	S4	-102.5	1037	5670.5	2711	-494.5
	S5	578	3529.5	4699	6529	4279
	S6	1900.5	295	2243	5177.5	3428
	S7	-1450	-2619	-4264.5	-564	-1002
	S8	-674	-3686.5	-3923.5	-4092.5	-1415
B	S9	-966.5	-1952	-2345.5	-3017.5	-8.5
	S10	-1408	3592.5	2658.5	4000	5251.5
	S11	-1170	-3521	4613	6714.5	6195.5
	S12	1463	128.5	8059.5	10275.5	10443.5

	S13	-1692	-2855	5586	3182.5	2651
	S14	623	2360	-1249	17	-1693
	S15	-1077	582	3235	-2224.5	-3547
	S16	-1162	-1829	-1770	-4989.5	-4660.5
C	S17	-806.5	-836.5	-655.5	-531	-406
	S18	-292.5	-377	440.5	553	1271
	S19	-440	-1390.5	1461	2074.5	3085
	S20	-922.5	-406.5	140.5	579	-788.5
	S21	-128	-1216	425.5	504	1972
	S22	-5663.5	-1431	-1489	-1388	-1259
	S23	-1044	-1731.5	-1027.5	-509	-979
	S24	-3409	-2199.5	-3777	-3259.5	-3377
D	S25	-6878.5	-4646	-5917	-6117.5	-4422
	S26	-1114.5	-4404.5	-5052.5	-5166	2265.5
	S27	-3576.5	-2335	-2217.5	-1154.5	633
	S28	-5259	-375.5	1793	2254.5	-8855
	S29	-1594.5	-2507	-3865.5	1154	1224.5
	S30	1925.5	-4417.5	-6113.5	-7746	-7380
	S31	-4862.5	-3902	-4611.5	-6220	-2255
	S32	-6306	-3177	-2101	409.5	-4988
E	S33	-1006.5	345.5	-1549.5	-1178	-1582.5
	S34	-453.5	-619.5	-487.5	-785	205
	S35	-2347	707.5	895	-233.5	-2926
	S36	-2030.5	-4207	-3452.5	-2830	-1787.5
	S37	1026	-820.5	-162.5	-1032.5	-594
	S38	-535.5	-1938	-1732.5	-614	-531
	S39	-1999	-2826	-3291	-3900.5	-3848.5
	S40	-446	2580	2119	-2500.5	-1226.5
F	S41	1914.5	3500.5	5098	700.5	220.5
	S42	-3155	-1584.5	-2016	-3196.5	-3615
	S43	-2096	-1651.5	-2659.5	-3355.5	-1802.5
	S44	1093	-1858.5	-2396.5	-2109	44
	S45	-1101.5	-1730	-355.5	-1042.5	-762
	S46	-901.5	1202	457	382	-845
	S47	-3010	4353.5	-755.5	858.5	-3665.5
	S48	509	3648	-314	-439.5	-131.5
G	S49	-1268.5	-4018	-3281	-1901	-2924.5
	S50	1549.5	-2806	-2206.5	-726	-1662.5
	S51	-1658.5	-1457.5	-733.5	-1951	-2244.5
	S52	-1058	-810.5	-905.5	-723.5	-725
	S53	-963	-330	-443	-862	-703
	S54	-950.5	-577	-817.5	-934	-1001.5
	S55	-1190	-1025	-839	-525.5	-535

	S56	-166	-524.5	417.5	286.5	488
H	S57	282.5	-1303.5	1568	1448	1494.5
	S58	2141	-1733.5	2458	1527	1434.5
	S59	-3428	-2021	3314.5	3258	2244.5
	S60	-2313.5	-3273	2118.5	2536.5	3004.5
	S61	-1020	2173.5	1760	474	838
	S62	-3439.5	-5158	-2303	-5732	-5558
	S63	79.5	736.5	-2142.5	-7436	-5801
	S64	-936	187	-5353.5	-6675	-5643.5
I	S65	-1360.5	-184.5	-4840	-6154.5	-6184
	S66	-2036	-5389.5	-2199.5	-1885	-804
	S67	-991.5	-3840.5	-2409	-1858.5	-1583.5
	S68	2629	390.5	744.5	-1066	5218
	S69	-4727	824.5	1208.5	2707.5	-6196.5
	S70	2921.5	3175	2617.5	3750.5	-594.5
	S71	1085	-3715.5	-4966	-5464.5	3228.5
	S72	-2305.5	-266.5	548.5	-51	-1236
J	S73	-436.5	-169.5	-1423.5	-500	-806.5
	S74	-710	204.5	-2387	-309	1374
	S75	1126	1007	3775.5	-4603.5	1755.5
	S76	-1796.5	-20.5	755	-445	-2468.5
	S77	-1260	1509.5	2245	1860.5	3568.5
	S78	278	2451.5	2944.5	3107.5	31
	S79	-765	1203.5	429.5	1177	1777.5
	S80	1932.5	-1545.5	-2535	-2622.5	-949

Channel Belt and Meander Belt:

Table 6 details the active channel width (or channel belt) of the Indus River from 1972 to 2022. Figure 8 illustrates the composite river section along with the numerical values for meander belt width. The channel belt represents the area occupied by the river channel in each specific year. The widest channel was 2,608 m at reach B section 15 in 1972, while the narrowest was 29 m at reach H section 62 in 2002. Channel widths have fluctuated over the years: in 1972, widths ranged from 2,308 m to 430 m; in 1979, from 1,926 m to 284 m; in 1992, from 1,254 m to 237 m; in 2002, from 1,185 m to 29 m; in 2012, from 917 m to 123 m; and in 2022, from 1,235 m to 111 m. The channel width was at its broadest in 1972 but has gradually diminished due to sedimentation and reduced water flow, leading to instability in the riverbank land-use patterns (Table 7). The meander belt, defined as the area occupied by the river's migration over a given time period, was generated by merging channel belt data from six different years (1972 to 2022). The maximum meander belt width was 7,550 m at reach 9, while the minimum width was 1,001 m at reach 3. The average width of the meander belt is 4,272 m (Figure 9).

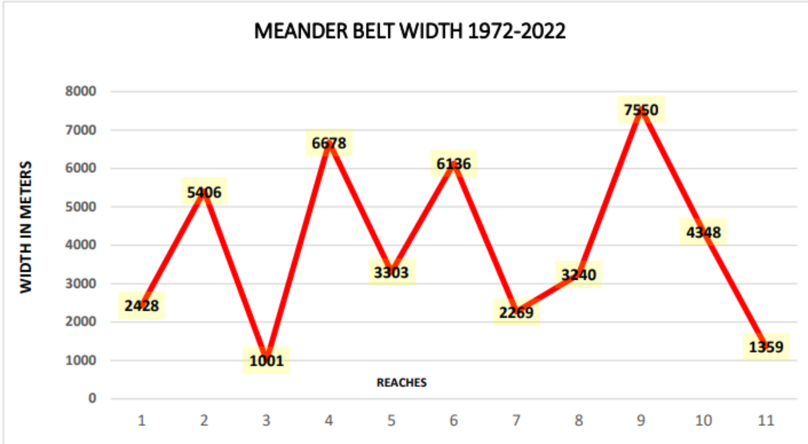

Figure 9: Meander belt trend on reaches

Table 5: Showing channel belt values of River Indus

REACHES	SECTION	WIDTH 1972	WIDTH 1979	WIDTH 1992	WIDTH 2002	WIDTH 2012	WIDTH 2022
A	S1	1359	788	776	1091	227	598
	S2	1132	862	824	231	255	305
	S3	1466	986	1050	1185	200	298
	S4	1341	696	736	233	275	734
	S5	1244	896	425	1065	377	369
	S6	1184	871	731	267	562	454
	S7	1556	674	734	371	215	393
	S8	1462	1926	897	374	517	689
B	S9	929	1322	610	899	324	705
	S10	1234	582	613	314	528	831
	S11	1224	1496	422	184	231	668
	S12	1009	1107	1254	357	364	529
	S13	1032	642	336	452	147	499
	S14	881	407	433	407	503	395
	S15	2308	1006	978	268	237	605
	S16	1348	730	882	678	237	206
C	S17	832	1109	774	577	463	357
	S18	597	722	914	313	437	179
	S19	1274	1102	375	211	150	328
	S20	1350	1045	938	555	577	588
	S21	844	620	472	117	323	479
	S22	862	579	237	229	281	249
	S23	665	711	582	341	443	189
	S24	1374	378	681	207	574	582
D	S25	1446	715	671	293	460	150
	S26	1006	607	656	505	353	366
	S27	1123	632	730	855	604	422
	S28	1035	835	376	322	279	451
	S29	1384	571	625	366	298	371
	S30	719	786	543	440	182	254
	S31	967	1418	358	345	435	1235
	S32	1062	284	560	142	525	609

E	S33	677	640	389	162	466	329
	S34	704	723	336	217	369	327
	S35	746	710	587	203	400	200
	S36	1882	601	483	368	896	639
	S37	1501	735	758	223	484	396
	S38	1114	371	829	140	488	506
	S39	1297	575	495	537	318	349
	S40	720	570	460	276	319	340
F	S41	840	725	420	514	313	358
	S42	1027	1135	398	228	185	207
	S43	864	446	873	392	355	296
	S44	1430	752	317	286	436	368
	S45	1563	982	530	273	422	482
	S46	793	942	818	444	194	520
	S47	590	450	379	326	317	216
	S48	736	1204	530	110	169	430
G	S49	1106	1439	783	267	811	208
	S50	1164	769	609	242	630	477
	S51	1389	500	551	116	362	111
	S52	1019	337	476	113	392	260
	S53	816	920	350	930	398	262
	S54	1015	306	352	259	433	326
	S55	1217	907	709	251	774	358
	S56	927	1013	322	239	864	202
H	S57	595	480	347	239	405	438
	S58	1223	399	742	296	736	197
	S59	1690	518	548	325	413	330
	S60	853	856	502	227	428	239
	S61	955	645	402	228	600	538
	S62	722	629	697	29	899	411
	S63	584	587	666	235	441	353
	S64	1317	713	309	198	886	231
I	S65	1086	1113	698	466	917	333
	S66	829	501	314	209	637	255
	S67	733	1108	1117	191	646	323
	S68	1202	680	555	646	792	230
	S69	1446	920	395	250	679	192
	S70	603	536	428	269	606	359
	S71	1056	536	321	317	512	281
	S72	896	1073	420	373	123	615
J	S73	924	837	532	387	539	640
	S74	826	1342	427	567	569	407
	S75	935	555	275	134	433	236
	S76	1491	290	421	193	539	270
	S77	1222	966	613	457	666	485

	S78	1244	1360	571	1182	551	241
	S79	430	832	719	742	424	367
	S80	896	895	528	342	247	421

Land Use Land Cover and Land Use land Cover Change:

Land Use Land Cover:

Land-use/land-cover (LULC) types within 30 km from the 1972 river centerline were analyzed for six selected years (Table 6). The results show an increase in built-up areas and a decrease in vegetation, while cultivated land, water bodies, and barren land fluctuated from 1972 to 2022. In 1972, agricultural land was at its maximum (4532 sq km), with minimum water bodies (407 sq km) and barren land (989 sq km). By 1979, water bodies were at their minimum (944 sq km), while built-up (3843 sq km) and uncultivated land (3797 sq km) were at their maximum. In 1992, uncultivated land peaked at 8580 sq km, with minimum water bodies (298 sq km) and barren land (518 sq km). In 2002, barren land was at its minimum (372 sq km), with maximum uncultivated (7098 sq km) and built-up areas (2833 sq km). By 2012, agricultural land reached its maximum (5862 sq km), with minimum water bodies (310 sq km) and barren land (538 sq km). In 2022, barren land was at its minimum (798 sq km), with maximum uncultivated (6090 sq km) and built-up areas (3787 sq km). These changes are illustrated in Figure 10 (a to d)

Table 6: LULC of Study area and its percentage from 1972 to 2022

LULC Class	1972		1979		1992		2002		2012		2022	
	Area (Sq km)	% of Area	Area (Sq km)	% of Area	Area (Sqkm)	% of Area	Area (Sqkm)	% of Area	Area (Sqkm)	% of Area	Area (Sq km)	% of Area
Agricultural Land	4534	29.54	2579	16.65	2147	14.61	1254	8.43	5862	39	2086	9
Barren Land	989	6.44	1049	6.77	518	3.53	372	2.5	588	3.91	798	5
Built-up Area	2457	16	3843	24.8	2512	18.3	2833	19.03	1368	9.1	3787	24
Uncultivated Land	5126	33.4	3797	24.51	8580	58.3	7096	47.66	3204	21.31	6090	29
Vegetation	1834	11.95	3281	21.18	647	4.4	942	6.32	3704	24.63	2084	13
Water	407	2.65	944	6.09	289	1.97	2391	16.06	310	2.06	1293	8

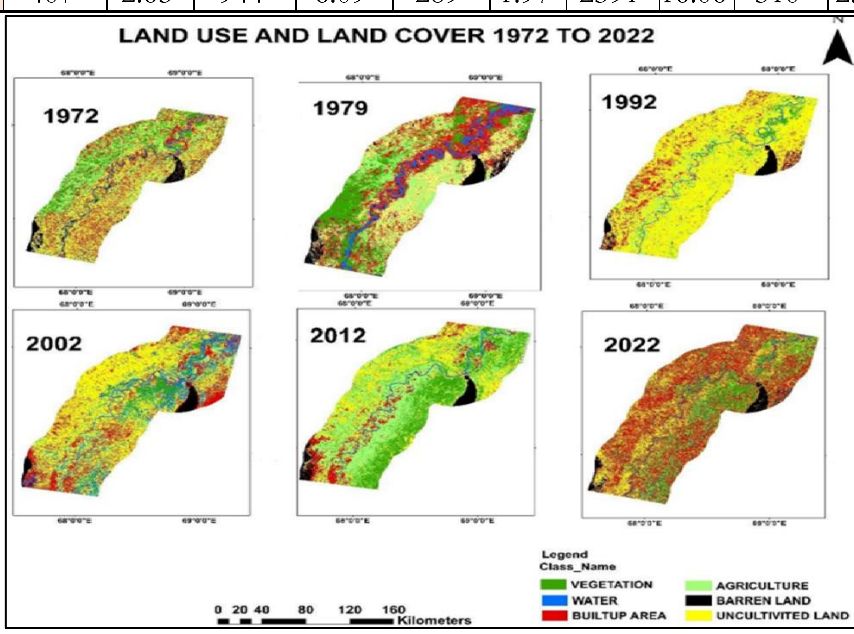

Figure 10: LULC maps of study area from 1972 to 2022

Land-use/Land-Cover (LULC) Change Detection:

To assess the impact of river shifting, land-use classified images were used for change detection from 1972 to 2012. Table 7 and Figures 11a–d show the land-use/land-cover change results for the selected area. The dynamic nature of the river has significantly altered the land-use types of its floodplain area. In 1972, the area was covered by 29.54% agricultural land, 6.44% barren land, 16% built-up area, 33.4% uncultivated land, 11.95% vegetation, and 2.64% water. By 1979, these areas had changed to 16.65%, 6.77%, 24.80%, 24.51%, 21.18%, and 6.09%, respectively. In 1992, the areas changed to 14.61%, 3.53%, 8.3%, 58.3%, 4.40%, and 1.97%. In 2002, the areas changed to 8.43%, 2.50%, 19.03%, 47.66%, 6.32%, and 16.06%. By 2012, the areas were 39%, 3.91%, 9.10%, 21.31%, 24.63%, and 2.06%, respectively.

LULC Change Percentages (1972-1979):

The land-use change detection revealed that 9.54% of agricultural land remained unchanged, with the rest converting to barren land (0.23%), built-up area (4.57%), uncultivated land (6.49%), vegetation (8.41%), and water (0.64%). For barren land, 3.55% remained unchanged, while the rest converted to agricultural land (0.06%), built-up area (1.08%), uncultivated land (0.77%), vegetation (0.24%), and water (0.58%). Of the built-up area, 7.75% remained unchanged, with the rest converting to agricultural land (2.36%), barren land (1.08%), uncultivated land (6.62%), vegetation (2.96%), and water (1.68%). Uncultivated land saw 9.56% remain unchanged, with the rest converting to agricultural land (3.36%), barren land (1.72%), built-up area (7.69%), vegetation (3.96%), and water (1.3%). Vegetation had 6.01% unchanged, with the rest converting to agricultural land (1.43%), barren land (0.05%), built-up area (2.63%), uncultivated land (1.23%), and water (0.53%). Finally, 1.12% of water remained unchanged, with the rest converting to agricultural land (0.04%), barren land (0.08%), built-up area (0.85%), uncultivated land (0.14%), and vegetation (0.38%).

LULC Change Percentages (1972-1992):

The land-use change detection revealed that 4.72% of agricultural land remained unchanged, with the rest converting to barren land (0.06%), built-up area (1.45%), uncultivated land (22.34%), vegetation (1.29%), and water (0.30%). For barren land, 2.67% remained unchanged, while the rest converted to agricultural land (0.30%), built-up area (0.73%), uncultivated land (1.93%), vegetation (0.08%), and water (0.16%). Of the built-up area, 2.83% remained unchanged, with the rest converting to agricultural land (2.88%), barren land (0.27%), uncultivated land (15.31%), vegetation (0.62%), and water (0.51%). Uncultivated land saw 18.71% remain unchanged, with the rest converting to agricultural land (3.83%), barren land (0.43%), built-up area (2.51%), vegetation (0.58%), and water (0.40%). Vegetation had 1.64% unchanged, with the rest converting to agricultural land (1.88%), barren land (0.04%), built-up area (2.25%), uncultivated land (6.29%), and water (0.26%). Finally, 0.36% of water remained unchanged, with the rest converting to agricultural land (0.56%), barren land (0.01%), built-up area (0.25%), uncultivated land (1.26%), and vegetation (0.27%).

LULC Change Percentages (1972-2002):

The land-use change detection revealed that 3.40% of agricultural land remained unchanged, with the rest converting to barren land (0.001%), built-up area (3.47%), uncultivated land (19.37%), vegetation (3.58%), and water (0.23%). For barren land, 2.32% remained unchanged, while the rest converted to agricultural land (0.09%), built-up area (1.36%), uncultivated land (2.09%), vegetation (0.16%), and water (0.06%). Of the built-up area, 5.58% remained unchanged, with the rest converting to agricultural land (2.01%), barren land (0.08%), uncultivated land (12.40%), vegetation (2%), and water (0.35%). Uncultivated land saw 15.57% remain unchanged, with the rest converting to agricultural land (1.64%), barren land (0.05%), built-up area (6.25%), vegetation (3.85%), and water (0.29%). Vegetation had 0.29% unchanged, with the rest converting to agricultural land (1.26%), barren land (0.001%), built-up area (1.50%), uncultivated land (8.19%), and water (0.27%). Finally, 0.29% of water remained unchanged, with the rest converting to agricultural land (0.33%), barren land (0.0001%), built-up area (0.51%), uncultivated land (1.30%), and vegetation (0.25%).

LULC Change Percentages (1972-2012):

The land-use change detection revealed that 12.64% of agricultural land remained unchanged, while the remainder was converted to barren land (0.21%), built-up areas (1.31%), uncultivated land (7.08%), vegetation (8.64%), and water (0.34%). For barren land, 2.67% remained unchanged, with the rest converting to agricultural land (1.02%), built-up areas (0.87%), uncultivated land (0.93%), vegetation (0.36%), and water (0.14%). Of the built-up areas, 2.41% remained unchanged, with the remainder converted to agricultural land (9.01%), barren land (0.28%), uncultivated land (4.61%), vegetation (5.78%), and water (0.48%). Uncultivated land saw 5.03% remain unchanged, with the rest converting to agricultural land (10.38%), barren land (0.61%), built-up areas (3.34%), vegetation (6.22%), and water (0.47%). Vegetation had 2.72% unchanged, with the rest converting to agricultural land (4.80%), barren land (0.09%), built-up areas (0.88%), uncultivated land (3.29%), and water (0.32%). Finally, 0.34% of water remained unchanged, with the rest converting to agricultural land (0.96%), barren land (0.01%), built-up areas (0.30%), uncultivated land (0.37%), and vegetation (0.64%).

Table 7: Land-cover changing percent during 1979, 1992, 2002 and 2012 with respect to 1972

		% of Agricultural Land	**% of Barren Land**	**% of Built up Area**	**% of Uncultivated Land**	**% of Vegetation**	**% of Water**
	1972						
1979	Agricultural Land	9.54	0.23	4.57	6.49	8.41	0.64
	Barren Land	0.06	3.55	1.08	0.77	0.24	0.58
	Built-up Area	2.36	1.08	7.75	6.62	2.96	1.68
	Uncultivated Land	3.36	1.72	7.69	9.56	3.26	1.3
	Vegetation	1.43	0.05	2.63	1.23	6.01	0.53
	Water	0.04	0.08	0.85	0.14	0.38	1.12
	1972						
1992	Agricultural Land	4.72	0.06	1.45	22.34	1.29	0.30
	Barren Land	0.30	2.67	0.73	1.93	0.08	0.16
	Built-up Area	2.88	0.27	2.83	15.31	0.62	0.51
	Uncultivated Land	3.83	0.43	2.51	18.71	0.58	0.40
	Vegetation	1.88	0.04	2.25	6.29	1.64	0.26
	Water	0.56	0.01	0.25	1.26	0.27	0.36
	1972						
2002	Agricultural Land	3.40	0.001	3.47	19.37	3.58	0.23
	Barren Land	0.09	2.32	1.36	2.09	0.16	0.06
	Built-up Area	2.01	0.08	5.58	12.40	2.00	0.35
	Uncultivated Land	1.64	0.05	6.25	15.57	2.85	0.29
	Vegetation	1.26	0.001	1.50	8.19	0.92	0.27
	Water	0.33	0.0001	0.51	1.30	0.25	0.29
	1972						
2012	Agricultural Land	12.64	0.21	1.31	7.08	8.64	0.34
	Barren Land	1.02	2.67	0.87	0.93	0.36	0.14
	Built-up Area	9.01	0.28	2.41	4.61	5.78	0.48
	Uncultivated Land	10.83	0.61	3.34	5.03	6.22	0.47
	Vegetation	4.80	0.09	0.88	3.29	2.72	0.32
	Water	0.96	0.01	0.30	0.37	0.64	0.34

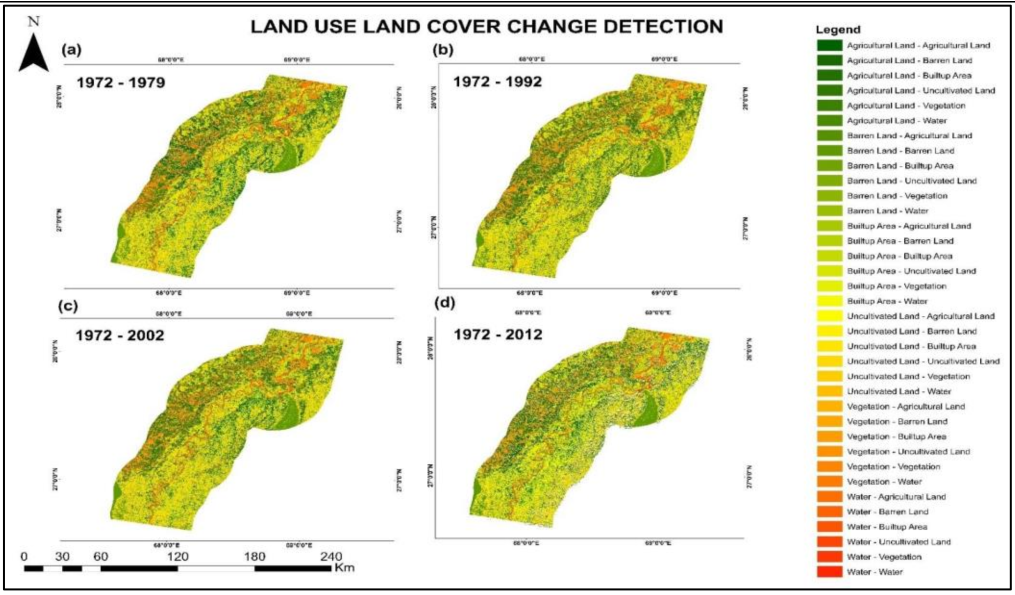

Figure 11: Land-use/land-cover change detection map from **a** 1972 to 1979, **b** 1972 to 1992, **c** 1972 to 2002 and **d** 1972 to 2012

Effect of River Dynamics on Land Use:

Erosion and deposition have significantly impacted agricultural land along the River Indus, with erosion increasing from 1972 to 2022. Deposition, particularly in river and waterbody areas, indicates active channel migration. Higher deposition was observed in agricultural areas, followed by grasslands and wetlands, which have shown a decreasing trend over the same period. Built-up areas have expanded from 1972 to 2022, reflecting population growth in the floodplains. Erosion and deposition have also affected settlement areas, leading to socio-economic stress due to the loss of homes and livelihoods, resulting in internal migration. The dynamic behavior of the river has caused modifications in land use and land cover (LULC) types, with agricultural land, vegetation, and built-up areas being chronically affected by river shifting. Cultivation remains prominent in the region, particularly within a 30 km buffer around the river, due to both erosion and accretion.

Discussion:

The study of land use and land cover changes around the River Indus from 1972 to 2022 illustrates the extensive alterations in the landscape over time. Urbanization and agricultural expansion have significantly transformed the region. These changes have likely increased runoff and sediment load in the river, affecting its flow and shape. The river's meandering has decreased over the years; it was highly sinuous in 1972 but much straighter by 2022. This change may be attributed to increased sedimentation and human activities disrupting the river's natural flow. Erosion and sediment deposition patterns in the river have varied over time. Between 1972 and 1979, the river eroded the left bank most significantly. From 1979 to 1992, sedimentation on the right bank increased. By 2002, erosion rates had diminished, and sediment deposition patterns had shifted. These patterns reveal how the river's shape and sediment dynamics have evolved. Channel migration reached up to 10,890 meters in 2022 in some areas, with the river shifting both left and right across different sections. This movement reflects both natural processes and human activities. Overall, the study highlights how land use changes and human activities have impacted the River Indus, making it straighter and altering its erosion and sedimentation patterns. These findings underscore the need for effective land and water management strategies to mitigate the impacts on the river and surrounding areas.

Conclusions:

- GIS and remote sensing techniques have proven to be highly effective for analyzing river shifting and dynamics.
- Certain river reaches, specifically A, B, C, H, I, and J, are particularly critical, showing significant migration and impact.
- The river's migration patterns vary along different reaches, with an overall trend of the river banks shifting more towards the left.
- Analysis of river sinuosity and channel width indicates that the river has become narrower over time, mainly due to sedimentation and reduced water flow.

- The relationship between land use changes and river dynamics is complex, with land use alterations significantly affecting river behavior.
- Effective flood management policies are essential to address the impacts on floodplain dwellers and to manage river systems sustainably.

References:

[1] Tariq, A., Shu, H., Kuriqi, A., Siddiqui, S., Gagnon, A. S., Lu, L., Linh, N. T. T., & Pham, Q. B. (2021). Characterization of the 2014 Indus river flood using hydraulic simulations and satellite images. Remote Sensing, 13(11), 2053.

[2] Kumar, A., & Srivastava, P. (2018). Landscape of the indus river. The Indian Rivers: Scientific and Socio-economic Aspects, 47-59.

[3] Raza, D., & Kidwai, A. A. (2018). Geospatial analysis of Indus River meandering and flow pattern from Chachran to Guddu Barrage, Pakistan. RADS Journal of Biological Research & Applied Sciences, 9(2), 67-74.

[4] Orengo, H. A., Knappett, C., & Knappett, C. (2018). Toward a definition of Minoan agro-pastoral landscapes: results of the survey at Palaikastro (Crete). American Journal of Archaeology, 122(3), 479-507.

[5] Dave, A. K., Courty, M.-A., Fitzsimmons, K. E., & Singhvi, A. K. (2019). Revisiting the contemporaneity of a mighty river and the Harappans: Archaeological, stratigraphic and chronometric constraints. Quaternary Geochronology, 49, 230-235.

[6] Mahar, G. A., & Zaigham, N. A. (2015). Examining spatio-temporal change detection in the Indus River Delta with the help of satellite data. Arabian Journal for Science and Engineering, 40, 1933-1946.

[7] Qureshi, M. N. (2021). Utilization of Natural Resources of Pakistan Quaid I Azam University].

[8] Inam, A., Clift, P. D., Giosan, L., Alizai, A., Kidwai, S., Shahzad, M. I., Zia, I., Nazeer, M., Khan, M. J., & Ali, S. S. (2022). The geographic, geological, and oceanographic setting of the Indus river–an update. Large Rivers: Geomorphology and Management, Second Edition, 488-520.

[9] Chakraborty, S. K. (2021). Riverine Ecology Volume 1: Eco-functionality of the Physical Environment of Rivers. Springer Nature.

[10] Mueller, J. E. (1968). An introduction to the hydraulic and topographic sinuosity indexes. Annals of the association of american geographers, 58(2), 371-385.

[11] Twisa, S., & Buchroithner, M. F. (2019). Land-use and land-cover (LULC) change detection in Wami River Basin, Tanzania. Land, 8(9), 136.

[12] Lambin, E. F., Turner, B. L., Geist, H. J., Agbola, S. B., Angelsen, A., Bruce, J. W., Coomes, O. T., Dirzo, R., Fischer, G., & Folke, C. (2001). The causes of land-use and land-cover change: moving beyond the myths. Global environmental change, 11(4), 261-269.

[13] Roy, N., & Sinha, R. (2018). Integrating channel form and processes in the Gangetic plains rivers: Implications for geomorphic diversity. Geomorphology, 302, 46-61.

[14] Lin, Y., Zhang, L., Wang, N., Zhang, X., Cen, Y., & Sun, X. (2020). A change detection method using spatial-temporal-spectral information from Landsat images. International Journal of Remote Sensing, 41(2), 772-793.

[15] Mamun, A., & Sobnam, M. (2021). Dynamics of Dharla River in Bangladesh relation to sinuosity and braiding: GIS-RS based spatial investigation. J. Appl. Geol. Geophys, 9(4), 50-56.